Measurement 174 (2021) 109000

Contents lists available at ScienceDirect

Measurement

journal homepage: www.elsevier.com/locate/measurement

Analysis of the voltage drop across the excitation coil for magnetic characterization of skin passed steel samples

Itsaso Artetxe [a,b], Fernando Arizti [a,b], Ane Martínez-de-Guerenu [a,b,*]

[a] CEIT-Basque Research and Technology Alliance (BRTA), Manuel Lardizabal 15, 20018 Donostia/San Sebastián, Spain
[b] Universidad de Navarra, Tecnun, Manuel Lardizabal 13, 20018 Donostia/San Sebastián, Spain

ARTICLE INFO

Keywords:
Distortion analysis
Permeability
Hysteresis loops
Electromagnetic measurements
Non-destructive testing
Skin pass

ABSTRACT

The distortion analysis of magnetic excitation (DAME) method has been recently proposed to facilitate magnetic measurements for non-destructive testing in which pick-up coils are not necessary. This method is based on the distortion effect that the permeability of the sample generates on the voltage across the excitation coil. The aims of the method presented in the present paper are to amplify this distortion effect using a current mode-controlled magnetization and to extract a distortion signal, of high signal-to-noise ratio (SNR), from the voltage measured in the excitation coil by means of a demodulation technique. This methodology is applied to different skin passed steels to characterize the elongation level, which is still a challenge for conventional non-destructive electromagnetic techniques. The relationships between the parameters derived from the distortion and from the hysteresis are studied. Measurements according to the DAME method are performed to verify the improvement in sensitivity for magnetic characterization.

1. Introduction

Electromagnetic methods such as eddy currents [1], the measurement of magnetic hysteresis loops [2], magnetic Barkhausen noise [3,4], or magnetic flux leakage [5] are widely used for defect detection or for characterizing mechanical and microstructural properties of ferromagnetic materials. Most of the electromagnetic systems used in laboratory are expensive and too slow to be of use on a line production [6–11]. Consequently, there are many authors working on developing systems and techniques that are implementable in industrial plants [1,12–17].

One of these systems is the commercial system 3MA (Micromagnetic Multiparameter, Microstructure and stress Analysis) which is based on some of the electromagnetic techniques mentioned previously and in the analysis of the distortion of the magnetic tangential field measured on the surface of the sample [18]. This system analyses the THD (Total Harmonic Distortion) factor, the amplitude of different harmonics and the coercive field named as H_{co}, which is the tangential field H value at the first zero place of the signal H without the fundamental frequency component after the remanence [19] and is correlated to the coercive field of hysteresis [19,20]. Other authors have studied the distortion of the magnetic tangential field analyzing its time derivative [21,22]. The influence of harmonics on hysteresis loops has also been analysed [23,24]. The distortion of the voltage measured in a pick-up coil has also been studied to characterize the stress of samples [25], to detect mechanical damage in pipelines [26] or to determine the phase composition of carbon in cast-iron [27].

In order to facilitate the development of robust, easy-to-implement and cost-effective systems for material magnetic characterization, Moorthy has proposed the distortion analysis of magnetic excitation (DAME) [28–31]. To the best of the authors' knowledge, until Moorthy's proposal to study the distortion of the magnetic excitation, only the distortion of the magnetic field measured on the surface of the sample or the distortion of the voltage measured in a pick-up coil have been analysed. One of the advantages of the DAME method is that the use of pick-up coils and their electronic conditioning stages are unnecessary, which simplifies the hardware of the measurement system. Moorthy has developed a system that measures the voltage in the excitation coil by using a current limiting resistor and by applying a triangular voltage over the excitation coil. The measured voltage is slightly distorted due to the permeability of the ferromagnetic sample placed in the magnetic circuit. To increase the resolution of the distortion, Moorthy calculates the time derivative of the magnetic excitation in refs. [28–31]. He plots this time derivative against the total applied voltage and names this plot as the DAME profile. Even though some parameters of the DAME profile

* Corresponding author.
E-mail address: amartinez@ceit.es (A. Martínez-de-Guerenu).

https://doi.org/10.1016/j.measurement.2021.109000
Received 5 November 2020; Received in revised form 23 December 2020; Accepted 5 January 2021
Available online 13 January 2021

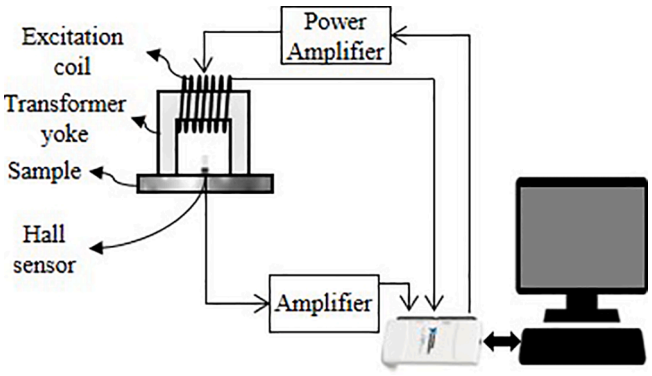

Fig. 1. Schematic block diagram of the setup for the analysis of the voltage drop across the excitation coil.

may be related to parameters derived from magnetic hysteresis loops, the relationship between the DAME profile and hysteresis loops or Barkhausen noise needs further study [30].

An interesting application of this method is the characterization of skin passed samples, as the magnetic characterization of industrial processes is still a challenge. Skin pass represents one of the final steps usually performed for the production of steel sheets after cold rolling and annealing. Skin pass rolling is a critical operation in the automotive industry to set a suitable degree of surface hardening, roughness and degree of flatness to the steel strips [32–34]. Moreover, skin pass is also applied to prevent stretcher strains (Lüder's bands), eliminating yield point elongation [35–37]. Compared with conventional rolling reduction, in skin pass the thickness reduction is generally under 2% [38].

Due to the importance of this steel processing step, some authors have developed models to predict the influence of the parameters of the skin pass rolling operation (rolling speed, force roll radius or rolling elongation) in the final mechanical properties of the strip (deformation [32,38], tensile [35], yield point elongation [36], hardness [39] or texture [40]). Other authors have characterized the final microstructural and mechanical properties of different skin passed samples with optical microscopy [34,41], Vickers micro hardness and tensile tests [39].

The relationship between microstructural, mechanical and magnetic properties makes electromagnetic non-destructive testing techniques suitable to verify the requirements of steel manufactures to perform in-situ monitoring of the whole steel production. Until now, the magnetic properties of samples after cold rolling reduction have been widely studied [4–6,24]. When deformation increases, the hysteresis losses and the coercive field increase [9,10,12,42] and the remanence and the permeability decrease [9,12,42]. Barkhausen noise is also sensitive to plastic deformation [10,12]. In the same way, the influence of rolling treatments on incremental permeability and eddy-current impedance has been studied [43]. A relationship between some parameters of incremental permeability and yield strength of steels has been established in [7]. The deformation state such as yielding, Lüders-strain and strain hardening have been studied by recently proposed new eddy current techniques [6]. However, despite the fact that some authors have studied the relationship between magnetic properties and rolling elongation in different steels [44], magnetic properties have yet to be completely exploited to monitor skin pass rolling.

The present paper proposes a new method to analyse the distortion effect of the permeability of the sample on the voltage drop measured across the excitation coil. The main differences with respect to the DAME method are the type of magnetization used and the signal processing that allows us to obtain a signal that accurately represents the distortion. The proposed method enabled us to characterize magnetically two sets of skin passed samples with different microstructural properties: interstitial free (IF) and dual phase (DP) steels. Moreover, since the permeability of the sample causes the analysed distortion, we

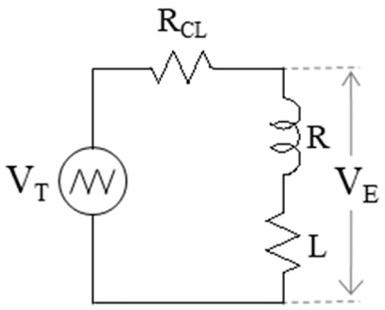

Fig. 2. Electrical equivalent circuit of the magnetizing circuit of the DAME method presented in [28–31]. R and L represent the resistance and the inductance, respectively, of the excitation coil.

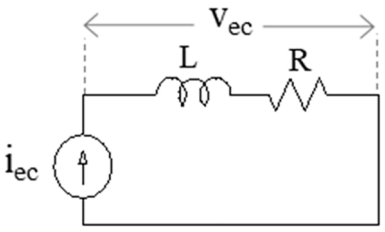

Fig. 3. Electrical equivalent circuit of the magnetizing circuit of the new method for the analysis of the voltage drop across the excitation coil.

compare the results of the proposed method with the results of direct measurements of hysteresis loops. Finally, as the DAME method is based on the same effect, we also measured and analysed skin passed samples according to the DAME method. The comparison analysis verified the improvement on the sensitivity to the skin pass elongation of the parameters derived from the distortion effect of the permeability on the voltage drop across the excitation coil relative to the DAME method.

2. Analysis of the voltage drop across the excitation coil

Fig. 1 represents a generic experimental setup to analyse the distortion effect on the voltage measured in the excitation coil. A U-shaped transformer yoke carrying the excitation coil magnetizes the sample when applying a time dependent excitation. The voltage drop across the excitation coil is acquired. The Hall sensor for the measurement of the magnetic tangential field is optional.

Specifically, to obtain the DAME profile, a triangular voltage V_T is applied over the excitation coil and a current limiting resistor R_{CL}, as shown in Fig. 2. The excitation coil is represented as the coil's resistance, R, and the inductance of the coil, L. The voltage across the excitation coil V_E is measured. Then, the time derivative of the voltage V_E is calculated. Finally, this time derivative is plotted against the total applied voltage V_T. This plot has been named in the previous literature as the DAME profile [28–31].

The measurement system proposed in the present paper is depicted in Fig. 3. It is slightly different to the DAME setup. In the measurement system proposed here, the magnetization is current-mode controlled; a sinusoidal current i_{ec} is applied directly to the excitation coil of the U-shaped transformer yoke.

The power amplifier generates the magnetizing current i_{ec}, which is a sinusoidal waveform of frequency ω_0 and amplitude I_0:

$$i_{ec} = I_0 sin(\omega_0 t) \tag{1}$$

Additionally, the tangential magnetic field H is measured on the sample surface with a Hall sensor. The voltage drop v_{ec} across the excitation coil is measured and can be expressed as [28–31]:

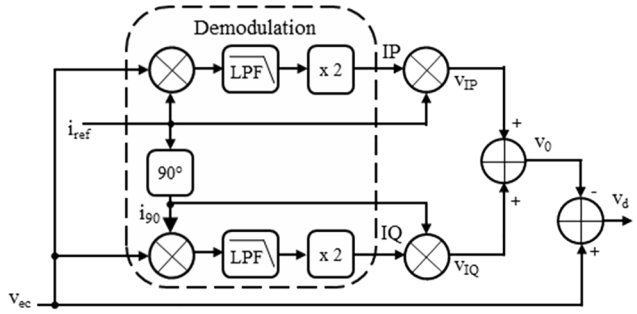

Fig. 4. Algorithm based on synchronous demodulation to calculate the signal v_d representative of the distortion effect of the permeability on the voltage v_{ec}.

$$v_{ec} = Ri_{ec} + \frac{dL}{dt}i_{ec} + L\frac{di_{ec}}{dt} \tag{2}$$

where R is the coil's resistance and L is the inductance of the coil, which can be expressed by:

$$L = \frac{N^2}{\frac{l_y}{A_y\mu_y\mu_0} + \frac{l_s}{A_s\mu_s\mu_0}} \tag{3}$$

where N is the number of turns of the excitation coil, l_y and l_s are the lengths of the magnetic flux path in the yoke and the sample, respectively; A_y and A_s are the cross sectional areas of the yoke and the sample, respectively; μ_y and μ_s are the relative permeabilities of the yoke and the sample, respectively; and μ_0 is the permeability of the vacuum. As the yoke and the sample are ferromagnetic materials, the relative permeabilities μ_y and μ_s are not constant as they vary with the applied alternating magnetizing field.

Assuming that the maximum permeability of the yoke is much larger than the maximum permeability of the sample and that the magnetic path length to the area relation is smaller in the yoke than in the sample, the inductance of the coil can be approximated to:

$$L \approx N^2\frac{A_s\mu_s\mu_0}{l_s} \tag{4}$$

Incorporating Eq. (4) into Eq. (2), v_{ec} can be expressed as a function of the permeability of the sample:

$$v_{ec} = Ri_{ec} + N^2\frac{A_s}{l_s}\frac{d\mu_s}{dt}\mu_0 i_{ec} + N^2\frac{A_s\mu_s\mu_0}{l_s}\frac{di_{ec}}{dt} \tag{5}$$

If the permeability of the sample was constant in time, and taking into account that the current i_{ec} is a sinusoidal waveform of frequency ω_0, the voltage v_{ec} would be a sinusoidal signal and thus, it would only have the fundamental frequency component ω_0. However, due to the non-linear behaviour of a ferromagnetic sample under an alternating magnetizing field, the permeability varies as a function of the applied field. This variable permeability introduces upper harmonic components generating a distortion in v_{ec}.

The effect of the permeability of the sample in the excitation coil's voltage, v_{ec}, when applying a controlled sinusoidal current, is analysed by eliminating the fundamental frequency component from v_{ec}. The resulting signal only contains the information of the upper harmonic components introduced by the non-linearity of the permeability of the sample, and it represents the distortion of the excitation voltage, which we denote as v_d in the following. The effect of the permeability of the sample on v_d will be analyzed in the next sections by representing v_d as a function of the magnetic tangential field strength H, measured by the Hall effect sensor. This representation will be named as v_d-H loop.

To calculate the signal v_d, representative of the effect of the permeability, we have implemented an algorithm based on synchronous demodulation, as detailed in Fig. 4. The steps of synchronous demodulation [45] are explained in Appendix A.

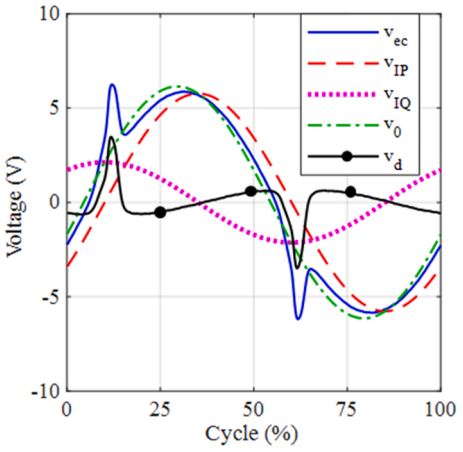

Fig. 5. An example of the voltage drop across the excitation coil (v_{ec}), the in-phase (v_{IP}) and in-quadrature (v_{IQ}) signals, the signal v_0 representative of the fundamental frequency component of v_{ec} and the signal v_d when measuring a ferromagnetic sample.

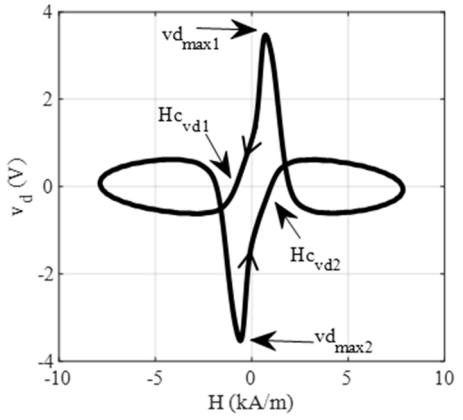

Fig. 6. An example of v_d-H loop when measuring a ferromagnetic sample.

We calculate the fundamental component of v_{ec}, as the in-phase, *IP*, and in-quadrature, *IQ*, amplitude components according to the synchronous demodulation (see (A6) and (A9) of the Appendix A). Then, the in-phase v_{IP} and in-quadrature v_{IQ} signals are generated by multiplying each component, *IP* and *IQ*, by the reference and in-quadrature signals, respectively, as:

$$v_{IP} = IPsin(\omega_0 t) \tag{6}$$

$$v_{IQ} = IQcos(\omega_0 t) \tag{7}$$

The signal v_0, which represents the fundamental component of v_{ec} is calculated by the sum of the two signals, v_{IP} and v_{IQ}:

$$v_0 = v_{IP} + v_{IQ} \tag{8}$$

To obtain the signal v_d, representative of the distortion, v_0 is removed from v_{ec}:

$$v_d = v_{ec} - v_0 \tag{9}$$

A comparison of these signals when measuring a ferromagnetic sample is shown as an example in Fig. 5. A generic signal v_{ec}, which represents the excitation coil's voltage when measuring a ferromagnetic sample, is plotted on a continuous blue line, together with the in-phase signal v_{IP}, on a dashed red line, the reference in-quadrature signal v_{IQ}, on a dotted magenta line; the signal v_0 on a continuous green line and the final signal v_d is represented with a continuous black line with dots. It can be seen by comparing the measured signal v_{ec} with v_d that the peak

Table 1
Elongation percentages of IF and DP sample sets.

Sample set	Elongation percentage ε (%)
IF	1.1 – 1.3 – 1.6–1.9 – 2.8–4.9–8.9
DP	0.4–0.6–0.9–1.2–1.7–2.2–4.2–8.2

of the distortion has become predominant in the signal v_d, which is one of the goals of the proposed methodology.

Finally, we plot the signal v_d against the magnetic field H to obtain a new representation, designated as the v_d-H loop, as shown in Fig. 6. Magnetic characterization of different samples can be performed by calculating parameters from the v_d-H loop like the amplitude of the peak of the signal v_d, vd_{max}, or the value of H nearest to zero when v_d is zero, Hc_{vd}. As v_d-H loop is antisymmetric, in Fig. 6 the negative and positive values of vd_{max} and Hc_{vd} are indicated. The parameter vd_{max} is calculated as the mean of the absolute values of vd_{max1}, the positive value, and vd_{max2}, the negative value, marked in Fig. 6. The parameter Hc_{vd} is calculated as the mean of the absolute values of Hc_{vd1} and Hc_{vd2}, marked in Fig. 6. When the applied varying current decreases in time from the maximum positive amplitude to the minimum negative amplitude (the corresponding descending branch of the conventional hysteresis loop), the value of H when v_d is zero for the first time is the parameter Hc_{vd1}, the negative value of Hc_{vd}. When the applied varying current increases in time from the minimum negative amplitude to the maximum positive amplitude (the corresponding ascending branch of the conventional hysteresis loop), the value of H when v_d is zero for the first time is the parameter Hc_{vd2}, the positive value of Hc_{vd}.

3. Materials and magnetic measurements

Skin passed samples previously prepared from commercial galvanized steels, IF-260 interstitial free (IF) and DP-600 dual phase (DP) steels [44] were used in the present study. Original samples prior to online skin passing could not be extracted. Therefore, there is no baseline skin pass deformation measurement for the samples. The skin pass rolling was performed in the longitudinal direction of the samples at the pilot plant of SZMF. The elongations were cumulative to the initial elongations from finishing in the line, which were 0.9% and 0.2% for IF and DP samples, respectively. The skin pass elongation percentages, ε, were calculated from the average of 8 thickness measurements (resolution of μm). Table 1 shows the final elongation percentages. Smaller sections were machined from the laboratory skin pass samples for magnetic testing. The magnetic test samples are 18 mm in width, with lengths ranging from 130 mm to 150 mm and final thicknesses ranging from 0.877 mm to 1.005 mm. The machined samples had their longitudinal direction in the rolling direction of the original samples and the magnetic measurements were made in the longitudinal direction. These samples were magnetically characterized previously in Ref. [44] using hysteresis loop measurements, with an experimental setup that used an encircling coil wound around the sample [46].

For the analysis of the distortion effect of the permeability of the sample on the voltage drop across the excitation coil v_{ec}, four measurements were made at the centre of for each sample, in the rolling direction, with a sinusoidal magnetizing current waveform of ± 0.45 A at an excitation frequency of 10 Hz, with the configuration represented

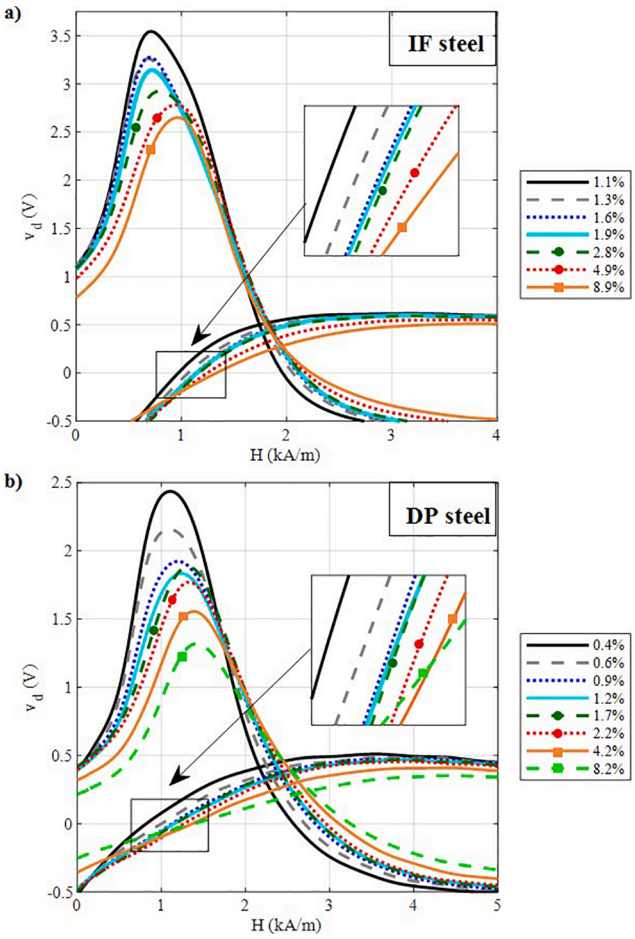

Fig. 8. Distortion signal v_d against magnetic induction H for a) IF and b) DP sample sets.

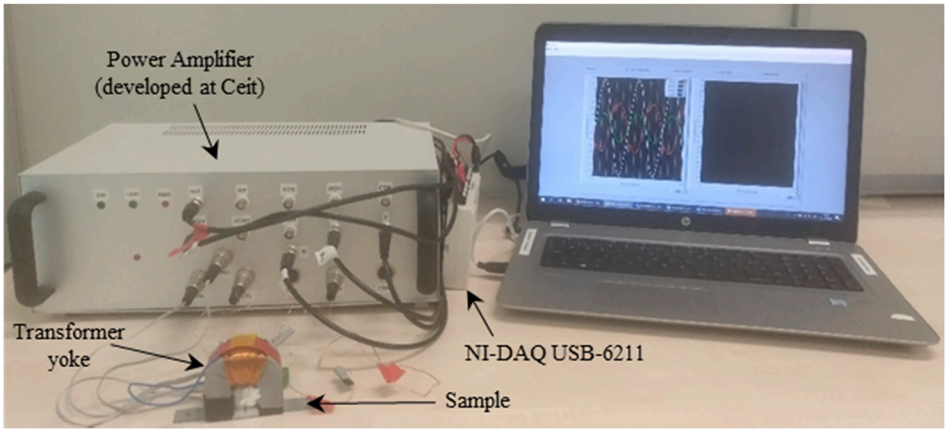

Fig. 7. Image of the experimental setup used for the analysis of the voltage drop across the excitation coil.

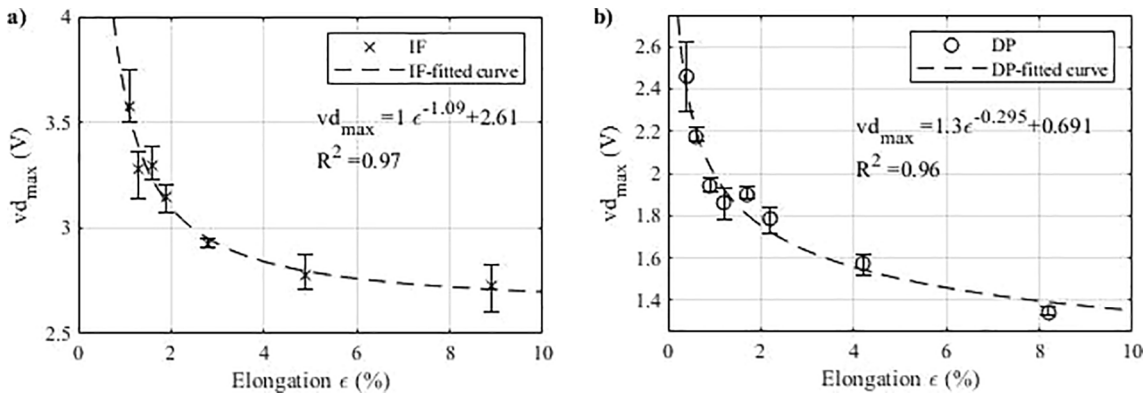

Fig. 9. Changes in vd_{max} for increasing elongation in (a) IF and (b) DP sample sets.

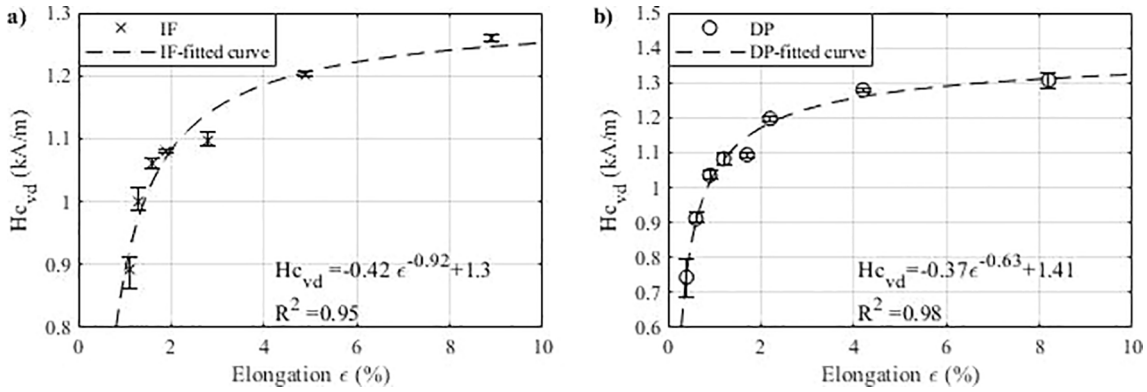

Fig. 10. Changes in Hc_{vd} for increasing elongation in (a) IF and (b) DP sample sets.

in Fig. 3. Then, the v_d-H loops were calculated according to the algorithm described in Fig. 4. The acquisition was performed with a DAQ-USB6211 commercial acquisition card of National Instruments. The material of the transformer yoke is grain oriented Fe - Si steel of a relative permeability of 30,000 at 1.5 T, the dimensions of its poles are 20 × 30 mm and the air gap between them is 20 mm. A picture of the experimental setup is shown in Fig. 7.

The v_d-H loop and the DAME profile methods are both based on the same effect. In order to compare the sensitivity of both methods, skin passed samples were also measured according to the DAME method [29,30] with the configuration represented in Fig. 2 and generating a triangular voltage V_T of ± 18 V at a frequency of 0.4 Hz. Four measurements were made at the centre of each sample in the rolling direction, and one without a sample.

4. Results

The first quadrant of the obtained v_d-H loops for the samples compiled in Table 1 is shown in Fig. 8. Although the amplitude of v_d of the IF sample set is greater than the one of the DP sample set, the change in the shape of the loop is similar for both materials. While the elongation level increases gradually, the amplitude vd_{max} decreases and Hc_{vd} increases.

The evolution of the maximum amplitude vd_{max} of the signal v_d with the elongation level is plotted in Fig. 9 for both materials. The parameter vd_{max} has been calculated by the mean of the absolute positive and negative values of vd_{max} shown in Fig. 6. The error bars represent the dispersion of the four measurements made in each sample. The fitting with a power function to data of IF (R^2 = 0.97) and DP (R^2 = 0.96) samples is good for both sets of samples.

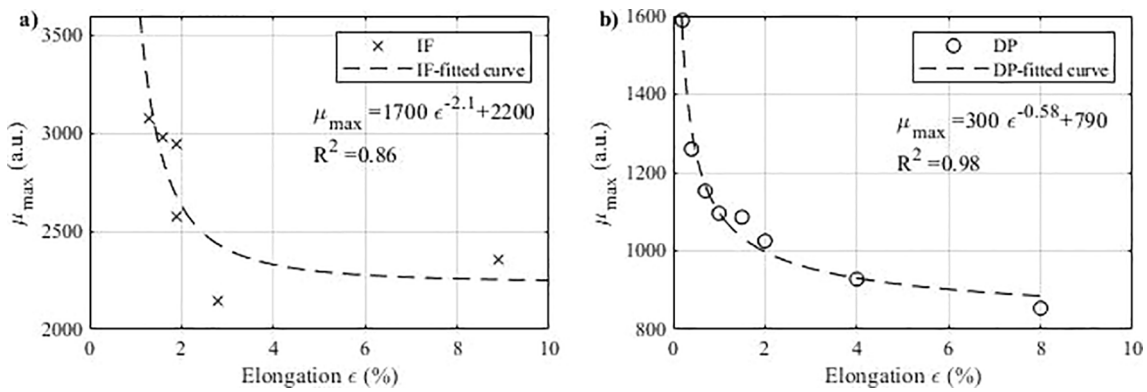

Fig. 11. Changes in μ_{max} for increasing elongation in (a) IF and (b) DP sample sets. Values of μ_{max} were calculated in [44].

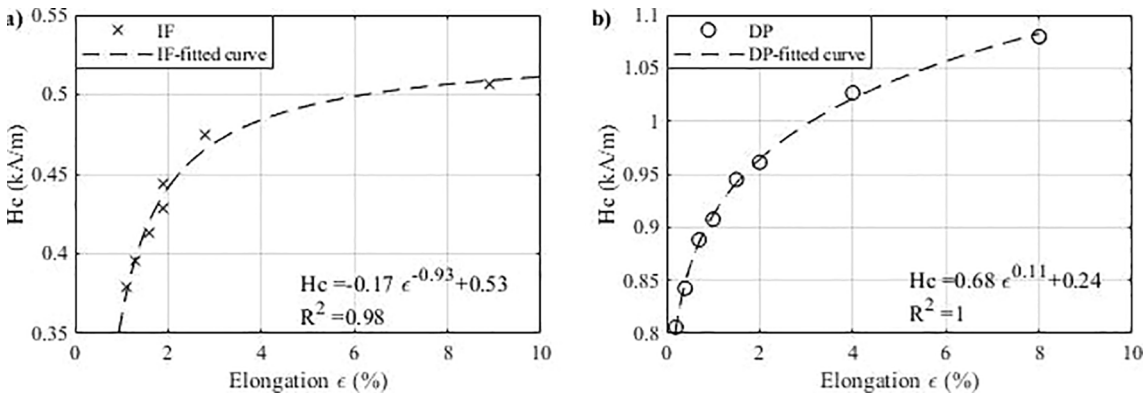

Fig. 12. Changes in *Hc* for increasing elongation in (a) IF and (b) DP sample sets. Values of *Hc* were calculated in [44].

Fig. 10 shows how the parameter Hc_{vd} changes with the elongation level, with the error bars which represent the dispersion of the four measurements made in each sample. The parameter Hc_{vd} has been calculated by the mean of the absolute positive and negative values of Hc_{vd} shown in Fig. 6. There is a large initial increase in Hc_{vd} and after an approximately 2% elongation, the curves level out. The fitting with a power function to data of IF and DP samples is good for both sets, where the fitting for the DP set is a slightly better than that for the IF sample set.

5. Discussion

As the signal v_d is representative of the distortion effect of the permeability of the sample on the voltage drop across the excitation coil, the relationship between the maximum amplitude v_{dmax}, derived from the v_d-H loop, and the maximum differential permeability μ_{max} parameter derived from hysteresis loops is studied. In addition, the relationship between the parameter Hc_{vd} and the coercive field of the hysteresis loop is analyzed. Finally, the DAME profiles of the same samples and their parameters are presented and compared with the parameters derived from the v_d-H loops to analyze the improvement in the sensitivity of the proposed method.

5.1. Relationship between v_d-H loop and hysteresis loop

Fig. 11 and Fig. 12 show the evolution of the parameters μ_{max} and *Hc* derived from hysteresis loops with the elongation, respectively. Values of μ_{max} and *Hc* of the IF and the DP sample sets were calculated in [44].

The maximum differential permeability μ_{max}, plotted in Fig. 11, decreases with the increase of the elongation in both materials. The range of this parameter is different in both materials, as the permeability of the IF samples is larger than the DP, showing that the IF is a much softer material, magnetically speaking. The fitting with a power function to data of DP samples ($R^2 = 0.98$) is better than the data of IF samples ($R^2 = 0.86$).

Fig. 12 shows how the parameter *Hc* presents a large initial increase with the elongation level and then, the curves level out. Other authors have analyzed this behaviour with the rolling elongation in the evolution of the coercive field, *Hc*, of the hysteresis loop. They attribute the initial slope of *Hc* to an increase in the mechanical hardness and the stabilization indicates the saturation of dislocation density [42,44,47]. As in Fig. 11 with μ_{max}, the range of *Hc* is different in both materials due to the sensitivity of this parameter to the microstructural properties of the IF and DP materials, specifically to the carbon content of the steel. The fitting with a power function to data of IF and DP samples is good for both sets.

The parameters vd_{max} and Hc_{vd} derived from the v_d-H loop undergo a similar evolution with the increase in the elongation level as the permeability and the coercive field derived from hysteresis loops, respectively. In fact, as the signal v_d represents the distortion of the voltage drop across the excitation coil caused by the permeability of the sample, a linear relationship between the signal v_d and the permeability derived from the hysteresis loop would be expectable. The parameter vd_{max} is plotted against the maximum differential permeability μ_{max} in Fig. 13, for IF and DP sample sets. The tendency shown in Fig. 13 confirms the relationship between vd_{max} and maximum differential permeability μ_{max}.

Similarly, the parameter Hc_{vd} is plotted against the coercive field *Hc* of hysteresis loops in Fig. 14 for IF and DP sample sets to analyze their relationships. The relationship between Hc_{vd} and *Hc* is linear for both sets of samples. These relationships confirm that the distortion is related to fundamental magnetic properties of the material under test. These relationships are of great importance to understand the influence of different mechanical and microstructural properties in the distortion of the voltage across the excitation coil because magnetic hysteresis has

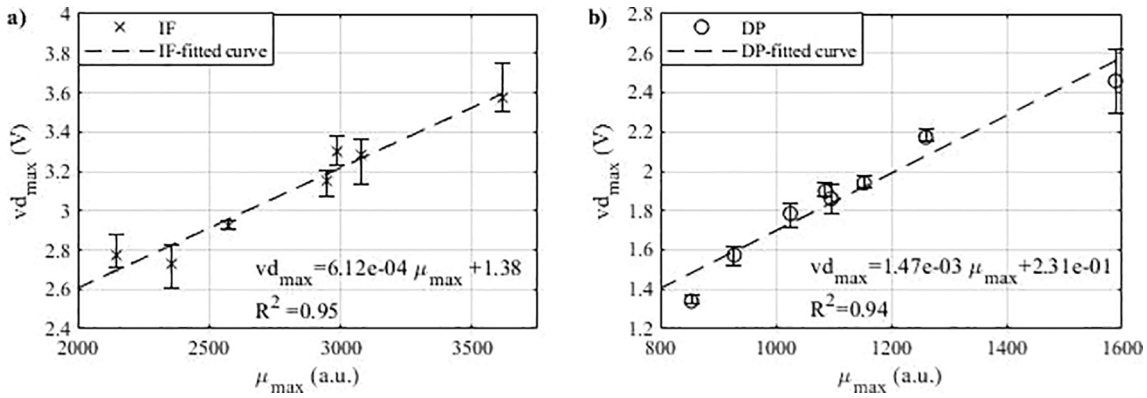

Fig. 13. Relationship between vd_{max} and maximum differential permeability μ_{max} in (a) IF and (b) DP sample sets. Values of μ_{max} were calculated in [44].

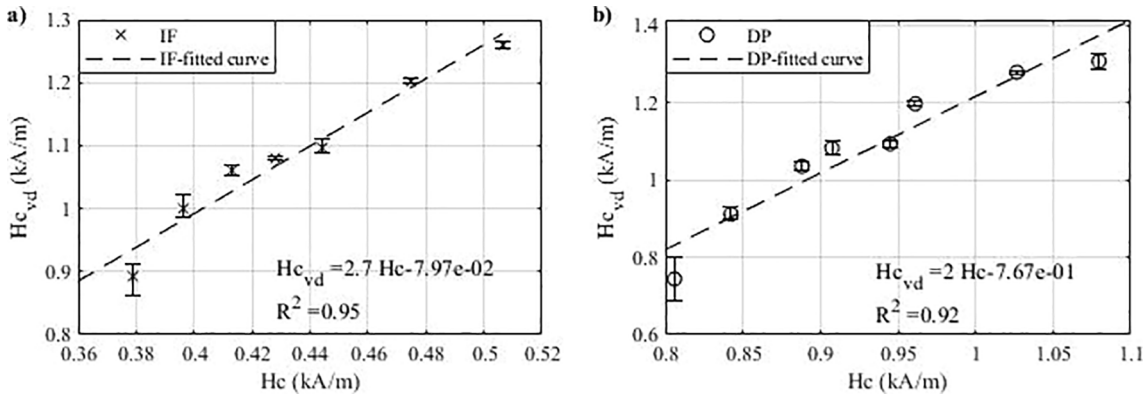

Fig. 14. Relationship between Hc_{vd} and Hc in (a) IF and (b) DP sample sets. Values of *Hc* were calculated in [44].

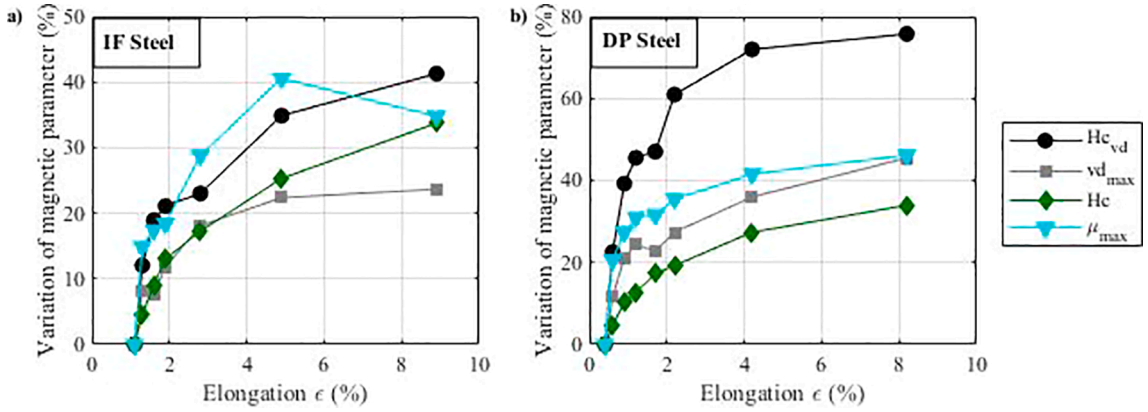

Fig. 15. The relative change of the magnetic parameters obtained from v_d-H loops and hysteresis loops [44] as a function of elongation in (a) IF and (b) DP sample sets.

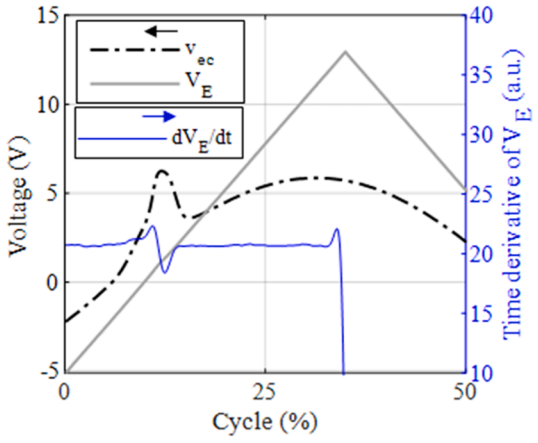

Fig. 16. Measured voltages across the excitation coil v_{ec} and V_E according to v_d-H and DAME methods respectively and time derivative of V_E.

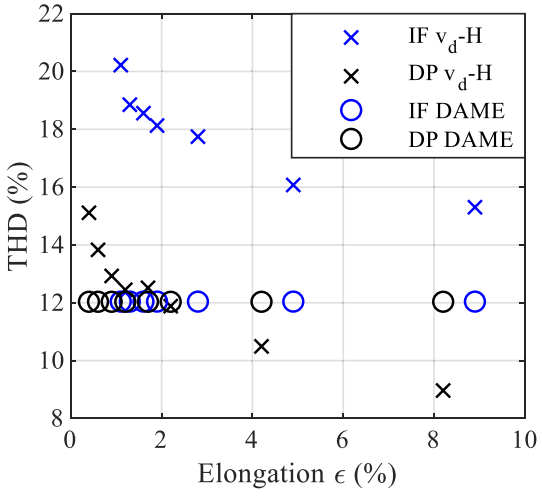

Fig. 17. Total Harmonic Distortion (THD) of the measured voltages v_{ec}, measured with the v_d-H method, and V_E, measured with the DAME method.

been widely studied.

Nevertheless, to compare the sensitivity to the skin pass elongation of the parameters derived from v_d-H loops and hysteresis loops, Fig. 15 shows the percentage of change of a given parameter *y* with respect to the reference sample y_0 (1.1% elongation in IF and 0.4% in DP), as proposed in [9] and it is calculated as:

$$\Delta y = 100 abs(y - y_0)/y_0 \tag{10}$$

where *y* is the mean value of a given parameter of a sample and y_0 is the mean value of the parameter of the reference sample.

The results of the IF set cannot be compared with the ones from the DP set because the reference is not the same for both of them. In the results of the IF set, in Fig. 15 a, there is no big difference between the parameters. Although μ_{max} shows a greater variation in intermediate elongation levels than Hc_{vd}, the variation of Hc_{vd} enables to characterize the whole range of skin pass elongation. For the DP steel set the most sensitive parameter is Hc_{vd} with a variation of 75%, as shown in Fig. 15

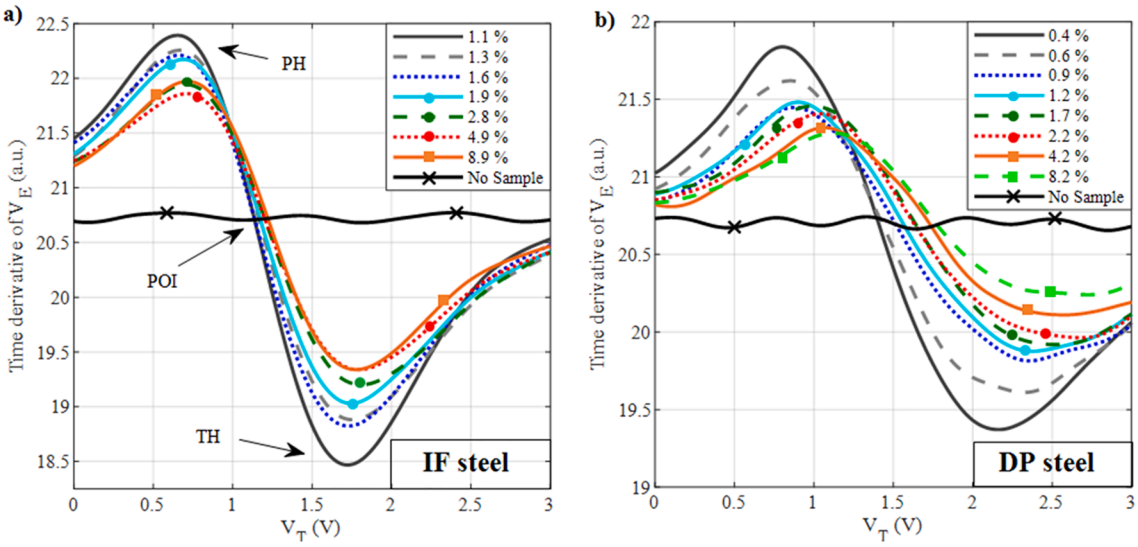

Fig. 18. DAME profile for (a) IF and (b) DP sample sets.

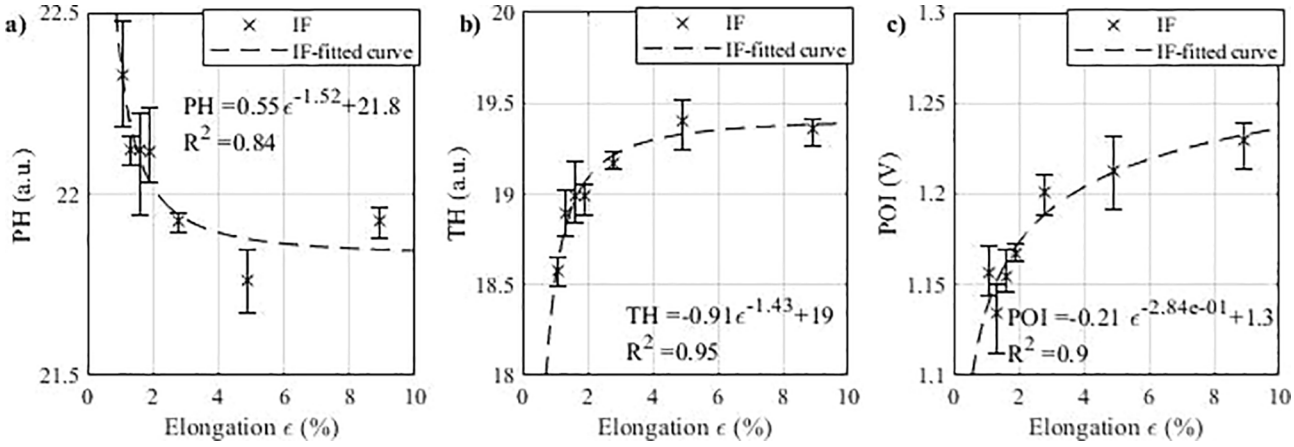

Fig. 19. Changes in (a) *PH*, (b) *TH* and (c) *POI* for increasing elongation in IF sample sets.

b. The similarity of the variations of vd_{max} and μ_{max} is again remarkable.

5.2. Comparison between v_d-H loop and DAME

For comparison purposes, both sample sets were also measured with the set up represented in Fig. 2 applying the DAME method described in Section 3. Fig. 16 compares the voltage v_{ec}, measured with the v_d-H method (see Fig. 3), and the voltage V_E, measured with the DAME method (see Fig. 2), when testing the IF sample of 0.2% of elongation. The distortion of v_{ec} is significant, whereas the distortion of V_E is almost

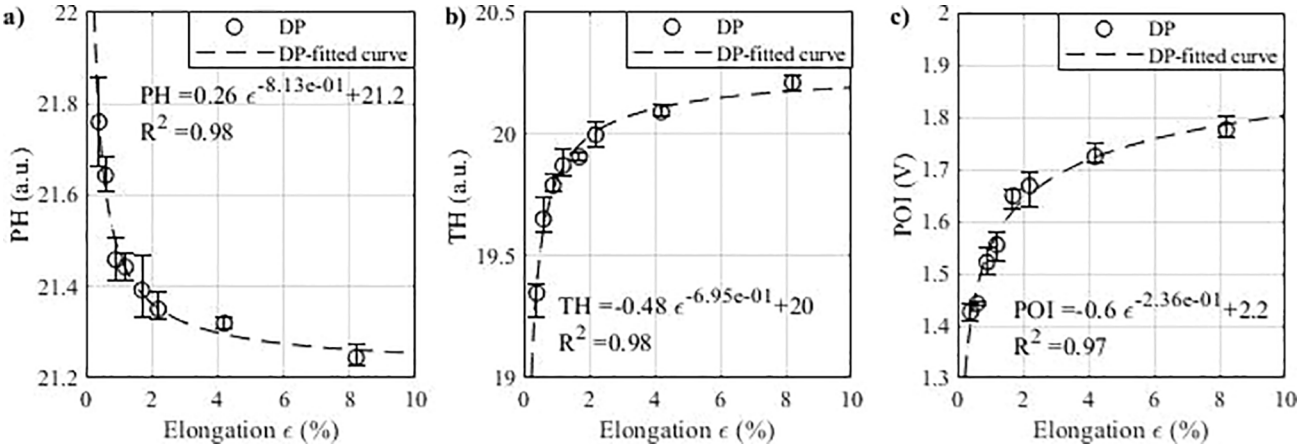

Fig. 20. Changes in (a) *PH*, (b) *TH* and (c) *POI* for increasing elongation in DP sample sets.

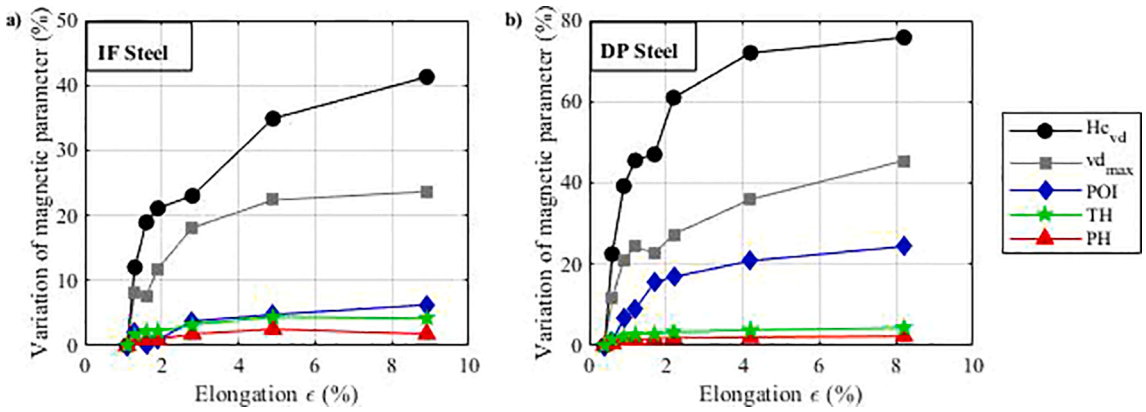

Fig. 21. The relative change of the magnetic parameters obtained from v_d-H loops and DAME profiles as a function of elongation in (a) IF and (b) DP sample sets.

imperceptible. The time derivative of V_E included in Fig. 16 shows the slight distortion of V_E.

This difference is also observed in Fig. 17 when we compare the total harmonic distortion (THD) factor of the voltage v_{ec}, measured when applying the v_d-H method, and of the voltage V_E, measured when applying the DAME method for the sample sets IF and DP. The THD of V_E voltages measured with the DAME method is nearly 12.1%, which is the typical THD of a triangular waveform. Thus, the influence of the sample in the THD is quite small. The THD of the measured v_{ec} signals changes with the elongation of the samples. Moreover, taking into consideration that the THD of an ideal sinusoidal waveform is 0%, all the samples generate a large distortion in the voltage v_{ec}. Therefore, the distortion effect on the voltage drop across the excitation coil due to the sample is amplified when the magnetization is current mode-controlled and sinusoidal.

The DAME profiles of the time derivative of magnetic excitation are plotted in Fig. 18 a, where the parameters derived from the DAME profiles defined in [30] are also indicated. These parameters are the peak height, *PH*, the trough height, *TH*, and the point of intersection of the DAME profiles with and without the sample, *POI*. In both materials, the effect of the elongation is approximately the same. When the elongation increases, the peak and trough decrease. However, the variation of *POI* in the DP steel set is greater than in the IF steel set.

In Fig. 19 and Fig. 20, the parameters derived from the DAME profiles, *PH*, *TH* and *POI*, are represented against the elongation percentage for IF and DP steels, respectively. Whereas there is a decrease with the elongation level in the *PH* parameter, the *TH* and *POI* parameters increase. Despite the fact that the coefficient of determination R^2 for a power curve fit is high for the three parameters, there is not enough resolution for elongations between 1.1 and 2% in IF samples and between 0.6 and 2.2% in DP samples.

The DAME profile is based on the same effect as the v_d-H loops, the distortion effect of the permeability of the sample on the voltage across the excitation coil. Therefore, comparing the results of DAME profiles with the results of the v_d-H loops is of great interest to observe the improvement of the analysis of the distortion effect. Comparing with the results of v_d-H loops, the parameter Hc_{vd} has better resolution for low elongation levels from 0.6% to 2.2% (see Fig. 10). Furthermore, the correlation between parameter Hc_{vd}, derived from v_d-H loop, with elongation is higher than the ones obtained with parameters derived from the DAME profile, especially in the IF set. For making a proper comparison, parameters derived from v_d-H loop and from DAME profile are given in relative units in Fig. 21 as proposed in [9]. For instance, the result of the Hc_{vd} measurement is given in kA/m, vd_{max} and *POI* in V and *PH* and *TH* are dimensionless values. Fig. 21 shows the variation percentage of the given parameter with respect to the reference sample (1.1% elongation in IF and 0.4% elongation in DP). The relative change observed in the parameters derived from the DAME profiles are less sensitive to the elongation levels than the parameters derived from v_d-H loops. Between the parameters derived from the DAME profile, the *POI* is the most sensitive parameter. Either way, the relative change in the magnetic parameters, due to skin pass rolling, reveal that the parameter Hc_{vd} of v_d-H loop is again the most sensitive parameter with a variation of 45% in IF and 90% in DP for the whole elongation range.

6. Conclusions

The distortion analysis of the voltage drop across the excitation coil, the v_d-H method, proposed here facilitates a quicker and simpler magnetic characterization of skin passed samples than the conventional magnetic methods of [6–9,18–22,44], which require low excitation frequency and complex and expensive instrumentation. The proposed method analyzes the voltage measured in the excitation coil, which reduces the use of sensors and the acquisition hardware facilitating its industrial implementation.

Furthermore, the magnetization mode and the analysis of the distortion are completely new compared with previous works [28–31]. Magnetization is conducted applying a controlled sinusoidal current directly on the excitation coil. The proposed way of magnetization amplifies the distortion caused by the permeability of the sample. The analysis of the distortion is performed extracting the signal v_d of high SNR from the voltage drop across the excitation coil. Finally, the v_d-H method consists of representing the v_d signal against the magnetic tangential field H to calculate new magnetic parameters, as Hc_{vd} and vd_{max}.

This methodology was used for the nondestructive magnetic characterization of skin passed samples. The parameters of the v_d-H cyle are capable of characterizing the elongation of skin passed samples of two different steels, IF and DP steels.

In addition, the linear relationship between parameters derived from v_d-H loops and from conventional hysteresis loops were also analyzed. This is quite relevant to understand the influence of the mechanical properties of the sample in the distortion of the measured voltage.

Moreover, the results obtained with the proposed method are better than the ones obtained with the DAME method, as it is posible to determine small elongation percentages (0.6–2.2%) with higher sensitivity in both sets of samples. Finally, the parameter Hc_{vd} derived from v_d-H loops shows to be the most sensitive parameter to the whole range of elongation of skin passed samples between all the magnetic parameters analyzed in the present study.

The main advantage of the analysis of the voltage drop across the excitation coil proposed in the present paper is that enables the non destructive characterization of small elongations of skin pass with a simplified system comparing to other electromagnetic techniques. This supposes a very interesting advance to facilitate the development of quality control and monitoring industrial systems based on

electromagnetic non-destructive testing. From the point of view of electromagnetism, although, the relationship of the distortion and the hysteresis loops has been analysed, further studies are needed to explain accurately this relationship and to understand why the Hc_{vd} parameter shows a better correlation than the ones derived from hysteresis loops to skin pass elongation. It would also be interesting to further analyse which is the behavior of the distortion effect when using electromagnetic yokes of different materials and geometries.

CRediT authorship contribution statement

Itsaso Artetxe: Conceptualization, Methodology, Software, Validation, Formal analysis, Investigation, Data curation, Writing - original draft, Writing - original draft, Writing - review & editing. **Fernando Arizti:** Conceptualization, Methodology, Validation, Resources, Writing - review & editing, Supervision. **Ane Martínez-de-Guerenu:** Conceptualization, Validation, Resources, Writing - review & editing, Supervision, Project administration, Funding acquisition.

Declaration of Competing Interest

The authors declare that they have no known competing financial interests or personal relationships that could have appeared to influence the work reported in this paper.

Acknowledgements

The authors acknowledge M. Stolzenberg from Salzgitter Mannesmann Forschung GmbH for the provision of the skin passed material, during the project under grant agreement no. RFSR-CT-2013-00031 of the European Union's Research Fund for Coal and Steel (RFCS) research program.

In addition, we acknowledge funding from the Basque Government under the Elkartek Program, project No. KK-2019/0010.

Appendix A. . Synchronous demodulation

For synchronous demodulation a reference signal i_{ref} at a fundamental frequency ω_0 and a signal in-quadrature, i_{90}, shifted 90° with respect to the reference signal i_{ref} are generated as:

$$i_{ref} = sin(\omega_0 t) \tag{A1}$$

$$i_{90} = cos(\omega_0 t) \tag{A2}$$

As an example, assuming that the signal to demodulate v_{in} only has the fundamental frequency component, it can be expressed as:

$$v_{in} = IPsin(\omega_0 t) + IQcos(\omega_0 t) \tag{A3}$$

where IP is the amplitude of the fundamental component in-phase with the reference i_{ref}, IQ is the amplitude of the fundamental component in-quadrature with the reference i_{ref} and t is time.

To calculate the amplitude IP, the signal v_{in} is multiplied by the reference i_{ref}:

$$p = i_{ref} v_{in} \tag{A4}$$

Including (A1) and (A3) in (A4), the product of i_{ref} and v_{in} can be expressed as:

$$p = \frac{IP}{2} - \frac{IP}{2} cos(2\omega_0 t) + \frac{IQ}{2} sin(2\omega_0 t) \tag{A5}$$

Then, the signal p is low-pass filtered (LPF) to eliminate frequency components greater than ω_0 and the result is half the in-phase amplitude IP. Therefore, IP can be calculated as:

$$IP = 2LPF(p) \tag{A6}$$

In the same way, to calculate the amplitude IQ, the signal v_{in} is multiplied by the reference signal shifted 90°, i_{90}:

$$q = i_{90} v_{in} \tag{A7}$$

Including expressions (A2) and (A3) in (A7), the product of i_{90} and v_{in} is:

$$q = \frac{IP}{2} sin(2\omega_0 t) + \frac{IQ}{2} + \frac{IQ}{2} cos(2\omega_0 t) \tag{A8}$$

The signal q is low-pass filtered to eliminate frequency components greater than ω_0 and the result is half the in-quadrature amplitude IQ. Therefore, IQ can be calculated as:

$$IQ = 2LPF(q) \tag{A9}$$

References

[1] N.M. Rodrigues, L.S. Rosado, P.M. Ramos, A portable embedded contactless system for the measurement of metallic material conductivity and lift-off, Measurement 111 (2017) 441–450.

[2] O. Stupakov, H. Kikuchi, T. Liu, T. Takagi, Applicability of local magnetic measurements, Measurement 42 (5) (2009) 706–710.

[3] X. Liu, W. Shang, C. He, R. Zhang, B. Wu, Simultaneous quantitative prediction of tensile stress, surface hardness and case depth in medium carbon steel rods based on multifunctional magnetic testing techniques, Measurement 128 (2018) 455–463.

[4] H. Dong, X. Liu, Y. Song, B.o. Wang, S. Chen, C. He, Quantitative evaluation of residual stress and surface hardness in deep drawn parts based on magnetic Barkhausen noise technology, Measurement 168 (2021) 108473, https://doi.org/10.1016/j.measurement.2020.108473.

[5] J.W. Wilson, G.Y. Tian, Pulsed electromagnetic methods for defect detection and characterisation, NDT and E Int. 40 (4) (2007) 275–283.

[6] T. Matsumoto, T. Uchimoto, T. Takagi, G. Dobmann, B. Ducharne, S. Oozono, H. Yuya, Investigation of electromagnetic nondestructive evaluation of residual

strain in low carbon steels using the eddy current magnetic signature (EC-MS) method, J. Magn. Magn. Mater. 479 (2019) 212–221.
[7] K. Li, L. Li, P. Wang, J. Liu, Y.u. Shi, Y. Zhen, S. Dong, A fast and non-destructive method to evaluate yield strength of cold-rolled steel via incremental permeability, J. Magn. Magn. Mater. 498 (2020) 166087, https://doi.org/10.1016/j.jmmm.2019.166087.
[8] M. Fanlin, L. Xiucheng, W. Heyun, H.e. Cunfu, W.u. Bin, Characterization of Elastic and Plastic Behaviors in Steel Plate Based on Eddy Current Technique Using a Portable Impedance Analyzer, Journal of Sensors 2017 (2017) 1–12.
[9] S. Takahashi, S. Kobayashi, I. Tomáš, L. Dupre, G. Vértesy, Comparison of magnetic nondestructive methods applied for inspection of steel degradation, NDT and E Int. 91 (2017) 54–60.
[10] D.L. Rodrigues-Jr, J.R.F. Silveira, G.J.L. Gerhardt, F.P. Missell, F.J.G. Landgraf, R. Machado, M.F. de Campos, Effect of Plastic Deformation on the Excess Loss of Electrical Steel, IEEE Trans. Magn. 48 (4) (2012) 1425–1428.
[11] R. Szewczyk, M. Nowicki, A. Ostaszewska-Liżewska, A. Bieńkowski, P. Nowak, M. Malinen, Accuracy of frame-shaped samples based measurements of magnetoelastic characteristics of soft magnetic materials, Measurement 162 (2020) 107899, https://doi.org/10.1016/j.measurement.2020.107899.
[12] G. Vértesy, I. Mészáros, I. Tomáš, Nondestructive magnetic characterization of TRIP steels, NDT and E Int. 54 (2013) 107–114.
[13] I. Tomas, G. Vertesy, Magnetic Adaptative Testing, Nondestruct. Test. Methods New Appl., InTech (2012) 145–186, https://doi.org/10.5772/2227.
[14] Y. Gabi, O. Martins, B. Wolter, B. Strass, Combination of electromagnetic measurements and FEM simulations for nondestructive determination of mechanical hardness, AIP Adv. 8 (4) (2018) 047502, https://doi.org/10.1063/1.4993669.
[15] K. Szielasko, I. Mironenko, I. Altpeter, H.-G. Herrmann, C. Boller, Minimalistic Devices and Sensors for Micromagnetic Materials Characterization, IEEE Trans. Magn. 49 (1) (2013) 101–104.
[16] J. Liu, J. Wilson, M. Strangwood, C.L. Davis, A. Peyton, J. Parker, Electromagnetic evaluation of the microstructure of Grade 91 tubes/pipes, Int. J. Press. Vessels Pip. 132-133 (2015) 65–71.
[17] O. Ortega-Labra, T.L. Manh, P. Martinez-Ortiz, J.M. Hallen, J.A. Perez-Benitez, A novel system for non-destructive evaluation of surface stress in pipelines using rotational continuous magnetic Barkhausen noise, Measurement 136 (2019) 761–774.
[18] G. Dobmann, Physical basics and industrial applications of 3MA -Micromagnetic Multiparameter Microstructure and stress Analysis, European Conf. Non-Destructive Test (ECNDT 2010) (2010) 1–6.
[19] G. Dobmann, H. Pitsch, Process and apparatus for the nondestructive measuring of magnetic properties of a test body, by detecting a tangential magnetic field and deriving harmonic components thereof, US5028869 (1991).
[20] Dobmann G, Pitsch H. Magnetic Tangential Field-Strength-Inspection, a Further NDT Tool for 3MA. Nondestruct. Charact. Mater., Springer Berlin Heidelberg; 1989, p. 636–43. doi:10.1007/978-3-642-84003-6_75.
[21] V. Moorthy, Unique correlation between non-linear distortion of tangential magnetic field and magnetic excitation voltage – Unexplored ferromagnetic phenomena and their application for ferromagnetic materials evaluation, J. Magn. Magn. Mater. 398 (2016) 101–108.
[22] G. Fillion, M. Lord, J.F. Bussière, Coercivity Measurement from Analysis of the Tangential Magnetic Field, Nondestruct. Charact. Mater. IV, Springer, US (1991) 223–230, https://doi.org/10.1007/978-1-4899-0670-0_27.
[23] S. Willcock, B. Tanner, Harmonic analysis of B-H loops, IEEE Trans. Magn. 19 (5) (1983) 2265–2270.
[24] S.N.M. Willcock, B.K. Tanner, The application of harmonic analysis to the magnetic properties of high-tensile steels, Mater. Lett. 4 (5-7) (1986) 307–312.
[25] H. Kwun, G.L. Burkhardt, Nondestructive measurement of stress in ferromagnetic steels using harmonic analysis of induced voltage, NDT Int. 20 (3) (1987) 167–171.
[26] G.L. Burkhardt, A.E. Crouch, Method and system for detecting and characterizing mechanical damage in pipelines using nonlinear harmonics techniques, US6239593B1 (1988).
[27] R.E. Ershov, A.J. Betenkova, T.G. Ivanenko, Testing cast-iron and steel by the upper harmonics magnetic method with simultaneous heating, NDT Int. 18 (4) (1985) 206–208.
[28] V. Moorthy, Distortion analysis of magnetic excitation – a novel method for non-destructive evaluation of depth of surface-hardening in ferritic steels, Philos. Mag. Lett. 94 (9) (2014) 564–572.
[29] V. Moorthy, Distortion Analysis of Magnetic Excitation - A novel approach for non-destructive microstructural evaluation of ferromagnetic steel, J Phys D Appl Phys 47 (2014), 202001, https://doi.org/10.1088/0022-3727/47/20/202001.
[30] V. Moorthy, Distortion analysis of magnetic excitation – Inherent reflection of properties of ferromagnetic materials, J. Magn. Magn. Mater. 382 (2015) 58–62.
[31] V. Moorthy, Distortion Analysis of Magnetic Excitation (DAME)-A Novel NDE Method for Evaluation of Properties of Ferromagnetic Materials, 19th World Conf, Non-Destructive Test. (WCNDT 2016) (2016) 1–8.
[32] H. Kijima, Influence of roll radius on contact condition and material deformation in skin-pass rolling of steel strip, J. Mater. Process. Technol. 213 (10) (2013) 1764–1771.
[33] H. Kijima, Influence of roll radius on roughness transfer in skin-pass rolling of steel strip, J. Mater. Process. Technol. 214 (5) (2014) 1111–1119.
[34] K. Hilgenberg, K. Steinhoff, Texturing of skin-pass rolls by pulsed laser dispersing, J. Mater. Process. Technol. 225 (2015) 84–92.
[35] D. Jafarlou, M. Hassan, N.A. Mardi, E. Zalnezhad, Influence of Temper Rolling on Tensile Property of Low Carbon Steel Sheets by Application of Hill 48 Anisotropic Yield Criterion, Procedia Eng. 81 (2014) 1222–1227.
[36] A.M. Giarola, P.H.R. Pereira, P.A. Stemler, A.E.M. Pertence, H.B. Campos, M.T. P. Aguilar, P.R. Cetlin, Strain heterogeneities in the rolling direction of steel sheets submitted to the skin pass: A finite element analysis, J. Mater. Process. Technol. 216 (2015) 234–247.
[37] A.I.Z. Farahat, A.M. Bahgat Gemeal, R.N. Elshaer, Influence of Skin Pass Design and Aging Phenomena on Steel Sheets Surface Characteristics, J Fail. Anal. and Preven. 16 (1) (2016) 86–94.
[38] M. Weiss, W. Ryan, B. Rolfe, C. Yang, The effect of skin passing on the material behavior of metal strip in pure bending and tension, AIP Conf Proc 1252 (2010) 896–902, https://doi.org/10.1063/1.3457651.
[39] J. Grassino, M. Vedani, G. Vimercati, G. Zanella, Effects of skin pass rolling parameters on mechanical properties of steels, Int. J. Precis. Eng. Manuf. 13 (11) (2012) 2017–2026.
[40] C. Wu, L. Zhang, P. Qu, S. Li, Z. Jiang, A new method for predicting the three-dimensional surface texture transfer in the skin pass rolling of metal strips, Wear 426-427 (2019) 1246–1264.
[41] M. Mehdi, Y. He, E.J. Hilinski, A. Edrisy, Effect of skin pass rolling reduction rate on the texture evolution of a non-oriented electrical steel after inclined cold rolling, J. Magn. Magn. Mater. 429 (2017) 148–160.
[42] M. Küpferling, C. Appino, V. Basso, G. Bertotti, F. Fiorillo, P. Meilland, Magnetic hysteresis in plastically deformed low-carbon steel laminations, J. Magn. Magn. Mater. 316 (2) (2007) e854–e857.
[43] M. Aghadavoudi-Jolfaei, J. Shen, A. Smith, L. Zhou, C.L. Davis, Non-destructive measurement of microstructure and tensile strength in varying thickness commercial DP steel strip using an EM sensor, J. Magn. Magn. Mater. 473 (2019) 477–483.
[44] A. Peyton, N. Karimian, J. Wilson, M. Stolzenberg, R. Schmidt, C. Davis, L. Zhou, P. Lombard, P. Meilland, A. Martinez-de-guerenu, K. Gurruchaga, The Application of Electromagnetic Measurements for the Assessment of Skin Passed Steel Samples, 19th World Conf. Non-Destructive Test. (WCNDT 2016), Munich, Germany (2016).
[45] C.S. Koukourlis, V.K. Trigonidis, J.N. Sahalos, Differential synchronous demodulation for small signal amplitude estimation, IEEE Trans. Instrum. Meas. 42 (1993) 926–931, https://doi.org/10.1109/19.252529.
[46] M. Soto, A. Martínez-de-Guerenu, K.K Gurruchaga, F. Arizti, A completely configurable digital system for simultaneous measurements of hysteresis loops and Barkhausen noise, IEEE Trans. Instrum. Meas. 58 (2009) 1746–1755, https://doi.org/10.1109/TIM.2009.2014510.
[47] H. Kikuchi, H. Murakami, K. Ara, Feasibility study for nondestructive evaluation of magnetic properties and hardness of two-layered specimens by magnetic single-yoke probe, NDT and E Int. 46 (2012) 1–6.